Hyperammonaemia disrupts daily rhythms reversibly by elevating glutamate in the central circadian pacemaker

Daniel Granados-Fuentes[1], **Kevin Cho**[2], **Gary J. Patti**[2], **Rodolfo Costa**[3,4,5], **Erik D. Herzog**[1,*], **Sara Montagnese**[5,6,*]

[1]Biology Department, Washington University in St. Louis, USA

[2]Center for Metabolomics and Isotope Tracing, Washington University in St. Louis, USA

[3]Department of Biology, University of Padova, Padova, Italy

[4]Institute of Neuroscience, National Research Council of Italy (CNR), Padova, Italy

[5]Chronobiology Section, Faculty of Health and Medical Sciences, University of Surrey, Guildford, UK

[6]Department of Medicine, University of Padova, Italy

Abstract

Patients with cirrhosis exhibit features of circadian disruption. Hyperammonaemia has been suggested to impair both homeostatic and circadian sleep regulation. Here, we tested if hyperammonaemia directly disrupts circadian rhythm generation in the central pacemaker, the suprachiasmatic nuclei (SCN) of the hypothalamus. Wheel-running activity was recorded from mice fed with a hyperammonaemic or normal diet for ~35 days in a 12:12 light-dark (LD) cycle followed by ~15 days in constant darkness (DD). The expression of the clock protein *PERIOD2* (PER2) was recorded from SCN explants before, during and after ammonia exposure, ± glutamate receptor antagonists. In LD, hyperammonaemic mice advanced their daily activity onset time by ~1 hour (16.8±0.3 vs. 18.1±0.04 h, p=0.009) and decreased their total activity, concentrating it during the first half of the night. In DD, hyperammonaemia reduced the amplitude of daily activity (551.5±27.7 vs. 724.9±59 counts, p=0.007), with no changes in circadian period. Ammonia (0.01 mM) rapidly and significantly reduced PER2 amplitude, and slightly increased circadian period. The decrease in PER2 amplitude correlated with decreased synchrony among circadian cells in the SCN and increased extracellular glutamate, which was rescued by AMPA glutamate receptor antagonists. These data suggest that hyperammonaemia affects circadian regulation of rest-activity behaviour by increasing extracellular glutamate in the SCN.

---

*Co-corresponding authors: **Correspondence to:** Prof. Sara Montagnese, Department of Medicine, University of Padova, Via Giustiniani 2, 35128 Padova, Italy, sara.montagnese@unipd.it, Office phone: 0039 (0)49 8218675; Prof. Erik D Herzog, Biology Department, Washington University at St. Louis, St. Louis, MO, USA, herzog@wustl.edu, Office phone: 001 314 935 8635.
Authors' contributions: <u>Daniel Granados-Fuentes</u>: experiments, procedures and design; data analysis and interpretation, writing of the article; <u>Kevin Cho</u>: experiments and procedures; data analysis and interpretation; <u>Gary J. Patti</u>: data analysis and interpretation, review of the article for important intellectual content; <u>Rodolfo Costa</u>: data analysis and interpretation, review of the article for important intellectual content; <u>Erik D. Herzog</u>: concept and design, data analysis and interpretation, review of the article for important intellectual content; <u>Sara Montagnese</u>: concept and design, data analysis and interpretation, writing of the article

Conflict of interest statement: none to declare

INTRODUCTION

Patients with cirrhosis exhibit features of central circadian disruption, with virtually unknown underlying mechanisms or consequences for therapy. For example, advanced liver disease is associated with parallel delays in the time of the daily peak of melatonin and cortisol [1–3], and reduced melatonin suppression by light at night [2]. These signs suggest impaired circadian response to light. Patients with severe hepatic encephalopathy (HE) can exhibit restless nights and daytime sleepiness, up to complete sleep-wake inversion [4, 5]. In addition, induced hyperammonaemia (i.e., by the oral administration of a mixture of amino acids that mimics bleeding-precipitated HE [6]) results in profound sleepiness [7] and an inability to generate deep, restful sleep in the subsequent sleep episode [8]. These observations have been interpreted as evidence for a role of hyperammonaemia in impinging on either homeostatic or circadian regulation of sleep cycles [9, 10].

The rhythmic output of the human central circadian clock has been traditionally attributed to the oscillation of approximately 20000 so-called clock neurons within the suprachiasmatic nuclei (SCN) of the hypothalamus. It is now accepted that SCN astrocytes also play a crucial role in generating mammalian circadian rhythmicity. Ablation of the essential clock gene *Bmal1* in mice SCN astrocytes lengthens the circadian period of clock gene expression in the SCN, and in locomotor activity behaviour [11]. This indicates that the rhythmic expression of clock genes in astrocytes contributes to the free-running periodicity of the mammalian master clock and modulates sleep-wake and other rhythmic phenotypes. Further studies have documented that SCN astrocytes: *i)* express clock genes in a rhythmic fashion; *ii)* show circadian Ca2+ oscillations with a broad night peak, in *quasi* antiphase with the sharper peak observed in SCN neurons in the day; *iii)* show circadian oscillations in glutamate release in phase with the Ca2+ peak [12–15]. Thus, SCN astrocytes function as a *bona fide* circadian clock, and the SCN overall output oscillation is the result of the *quasi* antiphasic oscillation of clock neurons and astrocytes. It is well established that hyperammonaemia causes both functional and morphological astrocyte abnormalities [16]). Therefore this study tested the potential of hyperammonaemia to act directly on the SCN to disrupt its output oscillation and, in turn, daily rhythms in physiology and behaviour.

MATERIALS AND METHODS

Animals

All animal procedures were approved by the Animal Care and Use Committee Guidelines from Washington University. We used homozygous Per2^LUC mice in which the *Luciferase* gene was fused to the endogenous mouse *Per2* gene, resulting in the production of a PERIOD2::LUCIFERASE fusion protein as a bioluminescent reporter of PER2 protein abundance [17]. Mice were obtained from Dr. J. Takahashi (Univ. Texas-SW) and maintained on the C57BL/6JN genetic background.

Wheel-running recordings

To record locomotor activity and generate the activity profiles, adult Per2^LUC mice (postnatal days 60 to 90; P60-P90) were placed individually in cages equipped with running-

wheels in light-tight chambers illuminated with fluorescent bulbs (~1.4 photons/cm^2/s [dim light]; General Electric). Wheel-running activity was recorded in 6-min bins (Clocklab Actimetrics) for ~35 days in a 12:12 h light-dark (LD) cycle (lights ON 6:00 am, lights OFF 6:00 pm) followed by ~15 days in constant darkness (DD). The period (i.e., the time after which a defined phase of the oscillation recurred) and amplitude (i.e., the difference between the maximum and the minimum value of the oscillation) of behavioural rhythmicity of each mouse was determined by χ^2 periodogram analysis [18] from the last 5 days in LD or DD from continuous recordings. At the end of the 15 days in DD, mice were returned to LD for eight days when we measured blood ammonia levels.

Hyperammonaemic diet

Standard food pellets (5058, Picolab mouse diet 20) were pulverized and mixed with ammonium acetate (Sigma-Aldrich) on a 20% w/w proportion with the appropriate amount of water to obtain a homogenous mixture which subsequently was formed into small pellets and dried as previously described [19, 20]. Blood ammonia levels with this diet increase approximately 3-fold [21], which is on par with levels observed in type C HE [22, 23]. Control mice were fed the same standard food pellets with no ammonium acetate added. Hyperammonaemic or control diet was available ad-lib throughout the wheel-running recording and was replaced every week with fresh pellets. Food consumption was measured every two days for four consecutive times at 2 PM during the light phase.

Determination of blood ammonia levels

At the end of wheel-running recordings, ammonia concentrations were measured with an ammonia sensor (Menarini diagnostics, Italy) from venous blood at 2:00 PM, 8 hours after daily light onset (Zeitgeber time 8, ZT 8) from mice consuming hyperammonaemic or normal diet. Briefly, 20 μl of venous blood were obtained via a capillary tube and transferred to a reagent strip and ammonia concentration was determined by reflectance [24].

Real-time PER2^{Luc} gene expression recordings

PER2 protein expression was recorded using real-time bioluminescence recording from SCN slices (300 μm, coronal) prepared from neonate (postnatal day 4; P4) or adult PER2^{LUC} mice (P60-P90) maintained in a 12:12 h light-dark (LD) cycle (lights ON 7:00 am, lights OFF 7:00 pm). Brains were quickly removed and chilled in Hanks' balanced solution (HBSS), supplemented with 0.01 M HEPES, 100 U/ml penicillin and 4 mM NaHCO$_3$. Slices were cut with a vibratome (EMS) and placed on 0.4 mm membrane inserts (Millipore) with 1 ml HEPES-buffered air-DMEM (1.2 ml) supplemented with 10% new-born calf serum (Invitrogen) and 0.1 mM beetle luciferin (Biosynth), the substrate for the PER2-luciferase reporter system. Petri dishes with the membrane inserts were sealed with vacuum grease and placed under photomultiplier tubes (PMT's H93319-11; Hamamatsu) at 36C in the dark. Bioluminescence was recorded in 10-min bins for at least 6 days. Peak-trough amplitude and circadian period of PER2^{LUC} were determined using Chronostar [25].

Cortical astrocyte cultures obtained from PER2^{LUC} mice (ages P2-6) were generated according to methods previously published [26]. Briefly, brains were placed in ice-cold HBBS supplemented with 100 U/ml penicillin, 100 μg/ml streptomycin, 10 mM HEPES

and 4mM NaHCO$_3$ (all from Sigma-Aldrich). Cerebral hemispheres were incubated in 1% DNase I, 0.005% trypsin and 0.002% EDTA (Invitrogen) at 37 °C for 15 min. Supernatant was forced through a sterile nylon mesh into 3 ml of horse serum (Invitrogen), centrifuged at 1000 rpm for 5 min and resuspended and plated in Dulbecco's Modified Eagle Medium (DMEM) supplemented with 10% fetal bovine serum (FBS) and 5% penicillin/streptomycin. Cells grew to confluence before passaging into new flasks. Astrocyte cultures between passage one and three were used for all experiments after approximately 1 month in vitro. PER2^{LUC} expression was recorded with PMT's.

Pharmacological experiments

For experiments blocking glutamatergic transmission, we used the AMPA receptor antagonists GYKI and NBQX (Tocris) both at a 100 μM final concentration. For experiments blocking excitatory amino acid transporters (EAAT1, EAAT2 and EAAT3) we used DL-TBOA (Tocris) at a 200 μM final concentration.

Dose-response curve to ammonia

To test the dose-response of the SCN to ammonia, ammonium acetate (Sigma-Aldrich) was dissolved in air-DMEM and used at 0.01, 0.1, 1, 5 and 10 mM final concentrations. We recorded PER2^{LUC} expression from neonatal and adult SCN with PMT's for 3 days and then added vehicle or ammonia to the media and recorded for at least 5 more days. Some cultures were then recorded following full-volume exchanges of the media to test for reversibility of ammonia effects.

PER2^{LUC} expression in single cells of SCN explants

PER2 expression in adult SCN explants was imaged on the stage of an inverted microscope (Nikon TE2000 fitted with a 20X objective and 0.5X coupler) inside a dark incubator (In Vivo Scientific). We added 0.1 mM beetle luciferin (Biosynth) to the medium and single cell bioluminescence was recorded at 36 °C with an ultrasensitive CCD camera (Andor Ixon or Ikon; 1x1 binning, 1-h exposures) for at least five days in vehicle-or ammonia-treated explants.

PER2^{LUC} single cells tracking and pixel analysis

To locate and track cellular bioluminescence, we used custom Python code [27] which identified potential cells in each frame using a standard difference of Gaussians blob detector. Briefly, the algorithm took the set of cell locations in each image and attempted to find spatial correspondences between them in the image time series. Then, raw signals from single cells were detrended and denoised and a Lomb-Scargle (LS) spectral analysis was performed. A sinusoid curve-fit with a constraint of +/−1 h of the LS peak period was performed to estimate rhythmicity including fitted period, phase, and amplitude. The power peak between 18-30 h was set to estimate the signal period. The synchronization index (SI) was calculated following the Kuramoto transformation. Additionally, a pixel analysis from the same movies was used to calculate percentage of pixels that were circadian and their instantaneous amplitudes and periods. Following pixel noise removal and multidimensional Gaussian filtering in SciPy tools using established methods [28], we generated time series

of pixel intensities and phase, amplitude and period maps of each SCN. The time series generated were then analysed for rhythmicity using MetaCycle [29]. Percentage of rhythmic pixels was calculated as [number of pixels reported by MetaCycle as significantly rhythmic (BH.Q < 0.01) with a period between 18h – 30 h / number of analysed pixels with non-zero pixel intensities]*100. Instantaneous amplitude, period and phases were measured by wavelet analysis using pyBOAT [30].

Glutamate release measured in SCN explants

To determine glutamate (Glu) levels in culture media from vehicle-and 5 mM ammonia-treated SCN explants, we used liquid chromatography/mass spectrometry (LC/MS) analysis. Adult PER2[LUC] SCN explants were cultured on membrane inserts in Petri dishes with SCN from 3 mice in each dish (n=6 control and 6 ammonia-treated). Using PER2 expression as a temporal marker, we collected SCN explants and their culture media after 3 days at either the peak or trough of daily PER2 expression (i.e., subjective midday or midnight, Circadian Time 6, CT6, or CT18). Briefly, SCN tissues were ground in a liquid nitrogen and dry ice bath. Protein abundance of each dish was determined by the BCA method. 1 μl of a methanol:acetonitrile:water mixture (2:2:1; Sigma-Aldrich: Thermo Scientific: Fisher LC/MS grade) per each 4 μg of protein was added. Samples were vortexed for 30 sec, incubated in liquid nitrogen for 1 min, allowed to thaw for 10 sec, and then sonicated at 25 °C for 10 minutes. This procedure was repeated 3 times. Samples were stored at −20 °C overnight and then centrifuged at 4 °C for 10 min at 14K RPM. The supernatant was transferred to LC vials and stored at −80 °C until LC/MS analysis. Culture media extraction was performed with 1:9 media:extract solvent (2:2:1 methanol:acetonitrile:water). The media were vortexed for 1 min, placed at −20 °C for an hour, and centrifuged at 4 °C for 10 min at 14K RPM. The supernatant was transferred to LC vials and stored at −80 °C until LC/MS analysis. Ultra-high performance LC (UHPLC)/MS was performed with a Thermo Scientific Vanquish Horizon UHPLC system interfaced with a Thermo Scientific Orbitrap ID-X Tribrid Mass Spectrometer (Waltham, MA). Hydrophilic interaction liquid chromatography (HILIC) separation was accomplished by using a HILICON iHILIC-(P) Classic column (Tvistevagen, Umea, Sweden) with the following specifications: 100 mm x 2.1 mm, 5 μm. Mobile-phase solvents were composed of A=20 mM ammonium bicarbonate, 0.1% ammonium hydroxide (adjusted to pH 9.2), and 2.5 μM medronic acid in water:acetonitrile (95:5); and B=acetonitrile:water (95:5). The column compartment was maintained at 45 °C for all experiments. The following linear gradient was applied at a flow rate of 250 μL min^{-1}: 0-1 min: 90% B, 1-12 min: 90-35% B, 12-12.5 min: 35-25% B, 12.5-14.5 min: 25% B. The column was re-equilibrated with 20 column volumes of 90% B. The injection volume was 4 μL for all experiments. Data were collected with the following settings: spray voltage, -3 kV; sheath gas, 35; auxiliary gas, 10; sweep gas, 1; ion transfer tube temperature, 275 °C; vaporizer temperature, 300 °C; mass range, 67-1500 Da, resolution, 120,000 (MS1), 30,000 (MS/MS); maximum injection time, 100 ms; isolation window, 1.6 Da . LC/MS data were processed and analysed with the open-source Skyline software [31]

Statistical analyses

Unless otherwise specified, comparisons between control and hyperammonaemic groups (or other comparisons between two independent groups) were performed by the Student's t test. Comparisons between more than two groups (i.e., concentrations of ammonia, or vehicle vs. ammonia vs. ammonia plus AMPA blockers) used one-way ANOVA (post-hoc: Tukey test) or two-way ANOVA. Unless otherwise specified, data are presented as mean±SEM, or %.

RESULTS

Hyperammonaemia impairs daily rest-activity rhythms in mice

To test the hypotheses that hyperammonaemia suffices to disrupt circadian rhythms in behaviour, we treated mice with a hyperammonaemic diet for two months. Venous ammonia levels increased about 50% (Fig. S1; 163.1±8.7 μg/dl vs. 102.4±11.2 μg/dl; p=0.003) with no change in mean food intake measured over four days (9.2±0.7 g in hyperammonaemic mice vs. 7.6±0.2 g in control mice; p=0.05). After a month in a light-dark cycle, hyperammonaemic mice had lower activity (19830±2514 counts per day) compared to controls (33882±4295 counts, p=0.03, Fig. 1 and Fig. S2) with similar results in constant darkness (19836±2369 hyperammonaemic, 31133±4077 control counts per day, p=0.02). Hyperammonaemic mice had reduced duration of daily locomotor activity in LD (7.6±0.7 h vs. 11.5±0.3 h control; p=0.0008) and DD (9.4±0.7 h vs. 11.8±0.5 h, p=0.02). Their ratio of time spent active each day (alpha) and resting (rho) was significantly lower (0.50±0.06 h) compared to controls in LD (1.00±0.04 h; p<0.0001) and in DD (0.70±0.07 h vs. 1.00±0.09 h, p=0.01) and their daily activity onset times were advanced (16.8±0.3 h) compared to control mice (18.1±0.04 h; p=0.009) (Fig. 1). In DD, hyperammonaemic mice also showed reduced circadian amplitude (551.5±27.7 vs. 724.9±59.0 arbitrary units; p=0.007) and no changes in their circadian period (23.6±0.1 h vs. 23.8±0.1 h, p=0.1).

Circadian rhythms of SCN are intrinsically sensitive to ammonia

To test if hyperammonaemia can directly modulate daily rhythms in the central circadian pacemaker, we recorded changes in the clock protein PER2, using real-time bioluminescence recordings from isolated SCN. Ammonia dose-dependently decreased amplitude of daily rhythms in PER2^{LUC} expression and increased circadian period in adult mouse SCN explants (Fig. 2). For example, PER2^{LUC} amplitude measured on day 2 after treatment was reduced significantly by doses at and above 0.1 mM (VEH, 108.4±11.1%; 0.01 mM 91.9±39.2%; 0.1 mM 42.7±4.2%; 1 mM 43.1±8.1%; 5 mM 54.9±8.7% and 10 mM 58.0±5.1%, p=0.002). Concentrations 0.1 mM ammonia increased circadian period in these cultures (VEH 24.2±0.2 h, 0.01 mM 24.4±0.3 h, 0.1 mM 25.1±0.2 h, 1 mM 25±0.05 h, 5 mM 25.3±0.3 h and 10 mM 25.2±0.2 h; p=0.003); 5 mM ammonia blunted circadian cycling in the adult SCN. These effects were reversible as removal of ammonia rapidly restored circadian amplitude PER2^{LUC} *in vitro* (Fig. 3). In contrast, the neonatal SCN and adult liver and skeletal muscle showed less sensitivity to ammonia *in vitro* (Figs. S3–5, p=0.5). Similar to the SCN in vitro following ammonia removal, SCN explanted from hyperammonaemic mice and cultured without ammonia showed normal PER2^{LUC} rhythms (Fig. S5). Daily rhythms intrinsic to the liver and skeletal muscle also showed no differences when cultured from mice that had consumed control or hyperammonaemic diet (Fig. S4).

These results indicate that ammonia rapidly, reversibly and specifically acts to reduce the coherent daily rhythms in the adult SCN, correlating with its effects on daily rhythms in rest-activity *in vivo*.

To evaluate if the ammonia-induced decrease in SCN amplitude reflects a loss of rhythms in individual SCN cells or an impairment in their ability to maintain synchrony, we recorded clock gene expression from individual cells within SCN explants. We found that, whereas control SCN cells tended to express their daily peak PER2 together, ammonia caused SCN cells to express a wide range of circadian periods and reduced their synchrony over many days (Fig. 4). These data indicate that cells remain circadian, but fail to synchronize, in the presence of elevated ammonia.

Circadian rhythms of astrocytes are intrinsically sensitive to ammonia

Following 5mM ammonia treatment, cultured cortical astrocytes showed a 50% reduction in circadian amplitude (Fig. S6, p<0.0001) and a shortened circadian period (24.7±0.04 h vehicle-vs. 23.2±0.2 h ammonia-treated, p=0.0003). These data implicate astrocytes as potential targets in abrogating the effects of ammonia on circadian rhythms.

Ammonia-induced circadian desynchrony depends on astrocyte-mediated glutamate uptake

Hyperammonaemia has been reported to elevate glutamate in the brain by blocking glutamate uptake by astrocytes [32]. To evaluate the mechanism of action of ammonia on the circadian system, we tested the hypothesis that ammonia exposure results in increased extracellular glutamatergic signalling in the SCN. We first evaluated whether glutamate receptor antagonists could reduce the effects of ammonia on SCN rhythms. We found that 100 μM AMPA receptor antagonists, 1-(4-Aminophenyl)-4-methyl-7,8-methylenedioxy-5H-2,3-benzodiazepine hydrochloride (GYKI), or 1,2,3,4-Tetrahydro-6-nitro-2,3-dioxo-benzo[f]quinoxaline-7-sulfonamide disodium salt hydrate (NBQX) blocked 5mM ammonia-induced changes of circadian amplitude in SCN explants (Fig. 5). Specifically, GYKI or NBQX administration during ammonia treatment resulted in SCN daily rhythms with amplitudes similar to vehicle treated SCN (p=0.2 for GYKI and p=0.4 for NBQX). GYKI or NBQX alone had no effect on circadian amplitude of the SCN (Fig. S7). We also found that GYKI prevented ammonia-induced desynchrony of circadian SCN cells (Figs. 4, 5 and S8). However, 100 μM GYKI did not fully rescue the hyperammonaemia-related increase in circadian period (Fig. 4F and S10).

To assess if ammonia-induced changes in the SCN are associated with changes in extracellular glutamate, we measured metabolite levels from culture media collected from SCN explants. LC/MS analysis revealed that, after being exposed to SCN cultures for 3 days in vitro, the media had lower glutamate levels around the peak (subjective dusk) than around the trough (subjective dawn) of SCN PER2 expression (28.4 ± 0.5 AU at CT12 vs. 46.2 ± 1.2 AU at CT6). This day-night difference was maintained in ammonia treated slices, but with a ~2.5-fold increase in extracellular glutamate levels (90.8±1.1 AU at CT12 and 118.9±1.7 AU at CT6; p<0.0001; Fig. S11).

Subsequently, we tested the hypothesis that ammonia blocks glutamate uptake by SCN astrocytes to disrupt circadian rhythms. We treated SCN explants with 200 μM DL-TBOA, a selective antagonist of excitatory amino acid transporters (EAAT1, EAAT2 and EAAT3) which elevates extracellular glutamate in the SCN [13]. We found that DL-TBOA decreased the amplitude of daily PER2 rhythms in the cultured SCN and to a similar extent to 5mM ammonia (p=0.1, Fig. 5). Importantly, we found that GYKI rescued coherent daily rhythms in the SCN from TBOA-induced amplitude reduction (p=0.01), implicating astrocytic excitatory amino acid transporters in ammonia's action on the SCN.

DISCUSSION

The results presented here suggest that when ammonia levels rise in the blood and brain, glutamate transporters fail to take up glutamate which accumulates and, through glutamate receptors in the SCN, disrupts synchrony among circadian cells and daily rhythms in behaviour. Of potential clinical relevance, we found that blocking AMPA glutamate receptors rescues the SCN from the effects of ammonia and high extracellular glutamate.

We found that hyperammonaemic mice advanced their daily activity onset by approximately an hour and decreased their total activity, concentrating it during the first half of the night. This is consistent with prior descriptions of decreased total locomotor activity in rats on a hyperammonaemic diet [33, 34] and with the decrease in total locomotor activity and disruption of the response to light described in another model of HE [35], rats after portocaval anastomosis [36].

Our results also are consistent with the observation that induced hyperammonaemia causes somnolence in both healthy volunteers and patients with cirrhosis [8], and reduced daily activity patients with cirrhosis [37]. However, actigraphy records from patients with cirrhosis are also characterized by increased night activity and delayed sleep-wake timing [37–39], which were not reflected in our model. This may depend on the differences between pure dietary-induced hyperammonaemia, i.e. our model [35], and hyperammonaemia associated with hepatic dysfunction, which characterises patients with cirrhosis. The use of the bile duct ligation model may help in this respect in future. Of interest, there is some evidence to suggest that insomnia (i.e., disturbed night sleep) is a feature of cirrhosis, while excessive daytime sleepiness is more specifically associated with HE and hyperammonaemia [7, 9, 40]

To our knowledge, the effect of ammonia on the SCN has never been previously tested. Ammonia decreased the amplitude of daily rhythms in PER2^{LUC} expression and increased its circadian period in adult mouse SCN explants. The highest ammonia concentration tested abolished daily rhythms in the SCN. The range of concentrations used in this study approximates those reached in the blood and/or cerebrospinal fluid of patients and animal models with clinically significant manifestations of hyperammonaemia [35]. In blood, these range between 70-500 μmol/L in chronic liver disease [40], while they can reach much higher values in patients with acute liver failure and children with urea cycle defects or inborn errors of metabolism [41]. Sleep-wake inversion has been generally associated with severe hyperammonaemia/HE [4, 5]. Of interest, the effects of ammonia (0.1-5mM) on the

SCN were fully reversible, as its removal rapidly restored circadian amplitude. This is in line with the clinical reversibility of HE and the sleep-wake abnormalities that are associated with it in response to ammonia lowering [42]. Further, cirrhosis-related abnormalities in the melatonin profile, which is a relevant SCN output in humans, have been shown to benefit from liver transplantation in one case report [43].

We found the neonatal SCN to be less sensitive to ammonia than the adult SCN. This is consistent with the observations that infants and young children (for example, those who suffer from urea cycle defects) tolerate considerably higher levels of ammonia compared to adults [44].

What mechanisms might underlie ammonia sensitivity in adults? Recent evidence indicates that the SCN encompasses a 'day active' neuronal clock and a 'night-active' astrocytic clock, which both contribute to coordination of SCN oscillations [11, 14]. We hypothesise that, in the adult SCN, ammonia-induced blockade of astrocytic uptake of glutamate leads to excessive glutamatergic signalling to SCN neurons and a loss of circadian synchrony. This was supported by evidence that blocking of excitatory amino acid transporters induced a decrease in amplitude like ammonia, that could be rescued by GYKI. It will be important to determine if the neonatal SCN is less sensitive to glutamate or depends on other signals to coordinate daily rhythms.

The discrepancy between ammonia-induced period changes in the adult SCN (where period increased) and cultured cortical astrocytes (where period decreased) may indicate that ammonia has differential effects on astrocytes and neurons, SCN and cortical cells, or other factors such as experimental conditions of the SCN cultured on a Millipore membrane compared to astrocytes plated on Petri dishes. As ammonia is expected to impinge mostly on astrocytes, the one presented here would be a virtually unique model of reversible astrocytic clock impairment within the SCN clock system. From a phenotypical stand-point, the observed increase in period length should be associated with a delay in the phase of sleep. This has been reported in patients with cirrhosis [9, 37–39] but does not seem to be strictly associated with HE/hyperammonaemia nor was it observed in hyperammonaemic mice in the present study. Finally, attempts at managing cirrhosis-related sleep-wake disturbance in the same way as delayed sleep phase disorder of central circadian origin [45], for example by administering light in the morning, have shown promise, especially in patients with mild liver disease [46, 47].

Ammonia increased extracellular glutamate levels in the SCN. As all neurons in the SCN are GABAergic, changes in glutamate levels have been attributed to the activity of astrocytes [13, 48, 49]. There are two known mechanisms by which hyperammonaemia might increase extracellular glutamate via astrocyte function: increased glutaminase levels and glutamate synthesis [50], and reduced function of glutamate transporters due to oxidative stress and reduced membrane expression [51]. Further, ammonia-dependent desynchronization was corrected by AMPA receptor antagonists. These antagonists did not prevent ammonia-dependent changes in period, which may reflect the relative amount of AMPA receptor density on neurons and astrocytes. Of interest, chronic exposure to ammonia has been previously shown to significantly reduce neuronal mRNA and protein

expression of AMPA glutamate receptors [52]. It has also been demonstrated that in rats chronic hyperammonemia alters the membrane expression of AMPA receptors in the hippocampus [53, 54] and the cerebellum [50]. Alternative explanations may be the fact that the blockade may also affect physiological glutamate functions and, given the significant desynchronization in response to ammonia, some degree of noise in period estimates (panels B and F of Figure 4). A non-competitive, highly selective AMPA receptor antagonist - a drug called perampanel – is available for medical use as an adjuvant for the treatment of epilepsy. In one case report in which it was used to treat drug-resistant epilepsy associated with advanced Alzheimer's disease (valproic acid, lacosamide and carbamazepine had not been effective), perampanel was shown to be beneficial also on the 'circadian rhythm disorder' exhibited by the patient [55]. While this is not extensively described in the case report, the authors most likely refer to the sleep-wake changes/tendency to sleep-wake inversion which characterise severe Alzheimer's disease.

While there is significant literature on NMDA glutamate receptor alterations in response to hyperammonaemia and their role in the pathophysiology of both persistent HE and acute liver failure-related HE [56], preliminary experiments suggested that their antagonists had stand-alone effects on SCN amplitude, precluding their use in our set of experiments.

In this study we opted for a model of pure hyperammonaemia in order for the observations *in vivo* (mice) and *in vitro* (explanted SCN) to match, and because we were specifically interested in the effects of hyperammonaemia on the astrocytic component of the master circadian clock. However, our model does not recapitulate a situation of hyperammonaemia added to the presence of liver disease for which bile duct ligation, for example, may be a more appropriate choice. On the other hand, the definition of the role of hyperammonaemia *per se* in the pathogenesis of sleep-wake abnormalities may help to start shedding light on the complex interactions between hyperammonaemia, liver synthetic dysfunction, enhanced GABAergic tone [57], systemic inflammation [58]), neuroinflammation [59] and portal-systemic shunting on the overall sleep-wake phenotype exhibited by patients with cirrhosis. Of interest, GABAergic tone modulation was recently shown to reduce subjective sleepiness and electroencephalographic slowing in patients with cirrhosis and mild HE [60], possibly leading to the hypothesis that the glutamate/GABA neurotransmission imbalance which is thought to underpin HE [61, 62] may have cumulative, negative effects on both the neuronal and astrocytic components of the master clock.

In conclusion, our data suggest that hyperammonaemia affects circadian regulation of rest-activity behaviour by increasing extracellular glutamate in the SCN. This is the first, direct proof of ammonia being implicated in central circadian disruption, and possibly also the first clinical model of astrocyte-dependent SCN output disturbance. The observed relationship between ammonia-dependent circadian disruption and glutamate levels, together with its response to glutamate receptor antagonists, may point to novel treatment strategies for the sleep-wake abnormalities associated with HE.

Supplementary Material

Refer to Web version on PubMed Central for supplementary material.

Funding

Data availability statement:

data will be made available on request to the co-corresponding authors

References

[1]. Steindl P, Finn B, Bendok B, Rothke S, Zee P, Blei A. Disruption of the Diurnal Rhythm of Plasma Melatonin in Cirrhosis. Clinical Trial Ann Intern Medicine 1995;123:274–277.

[2]. Montagnese S, Middleton B, Mani A, Skene D, Morgan M. On the origin and the consequences of circadian abnormalities in patients with cirrhosis. The American journal of gastroenterology 2010;105:1773–1781. [PubMed: 20332771]

[3]. Montagnese S, Middleton B, Mani A, Skene D, Morgan M. Changes in the 24-h plasma cortisol rhythm in patients with cirrhosis. Journal of hepatology 2011;54.

[4]. Sherlock SS WH White LP; Phear EA. Portal-systemic encephalopathy; neurological complications of liver disease. Lancet (London, England) 1954;267:454–457. [PubMed: 13193045]

[5]. Kurtz D, Zenglein J, Imler M, Girardel M, Grinspan G, Peter B, et al. Night sleep in porto-caval encephalopathy. Electroencephalography and clinical neurophysiology 1972;33:167–178. [PubMed: 4114153]

[6]. Douglass AAM H, Record C Amino acid challenge in patients with cirrhosis: a model for the assessment of treatments for hepatic encephalopathy. Journal of hepatology 2001;34:658–664. [PubMed: 11434611]

[7]. Kann A, Ba-Ali S, Seidelin J, Larsen F, Hamann S, Bjerring P. The effect of induced hyperammonaemia on sleep and melanopsin-mediated pupillary light response in patients with liver cirrhosis: A single-blinded randomized crossover trial. PloS one 2022;17.

[8]. Bersagliere AR ID Nardi M; Schiff S; Gatta A Amodio P; Achermann P Montagnese S. Induced hyperammonemia may compromise the ability to generate restful sleep in patients with cirrhosis - Bersagliere - 2012 - Hepatology - Wiley Online Library. Hepatology 2012;55:869–878. [PubMed: 21994139]

[9]. Córdoba J, Cabrera J, Lataif L, Penev P, Zee P, Blei A. High prevalence of sleep disturbance in cirrhosis. Hepatology (Baltimore, Md) 1998;27:339–345.

[10]. Marjot T, Ray D, Williams F, Tomlinson J, Armstrong M. Sleep and liver disease: a bidirectional relationship. The lancet Gastroenterology & hepatology 2021;6:850–863. [PubMed: 34273289]

[11]. Tso CS T; Greenlaw AC; Puri T; Mieda M; Herzog ED. Astrocytes Regulate Daily Rhythms in the Suprachiasmatic Nucleus and Behavior. Current biology 2017;27:1055–1061. [PubMed: 28343966]

[12]. Brancaccio M, Edwards M, Patton A, Smyllie N, Chesham J, Maywood E, et al. Cell-autonomous clock of astrocytes drives circadian behavior in mammals. Science (New York, NY) 2019;363:187–192.

[13]. Brancaccio M, Patton A, Chesham J, Maywood E, Hastings M. Astrocytes Control Circadian Timekeeping in the Suprachiasmatic Nucleus via Glutamatergic Signaling. Neuron 2017;93:1420–1435. [PubMed: 28285822]

[14]. Hastings M, Maywood E, Brancaccio M. The Mammalian Circadian Timing System and the Suprachiasmatic Nucleus as Its Pacemaker. Biology 2019;8.

[15]. Hastings M, Maywood E, Brancaccio M. Generation of circadian rhythms in the suprachiasmatic nucleus. Nat Rev Neurosci 2018;19:453–469. [PubMed: 29934559]

[16]. Norenberg M, Jayakumar A, Rama Rao K, Panickar K. New concepts in the mechanism of ammonia-induced astrocyte swelling. Metabolic brain disease 2007;22.

[17]. Yoo S, Yamazaki S, Lowrey P, Shimomura K, Ko C, Buhr E, et al. PERIOD2::LUCIFERASE real-time reporting of circadian dynamics reveals persistent circadian oscillations in mouse peripheral tissues. Proceedings of the National Academy of Sciences of the United States of America 2004;101.

[18]. Sokolove P, Bushell W. The chi square periodogram: its utility for analysis of circadian rhythms. Journal of theoretical biology 1978;72:131–160. [PubMed: 566361]

[19]. Felipo V, Miñana M, Grisolía S. Long-term ingestion of ammonium increases acetylglutamate and urea levels without affecting the amount of carbamoyl-phosphate synthase. European journal of biochemistry 1988;176:567–571. [PubMed: 3169014]

[20]. Marini S, Santangeli O, Saarelainen P, Middleton B, Chowdhury N, Skene D, et al. Abnormalities in the Polysomnographic, Adenosine and Metabolic Response to Sleep Deprivation in an Animal Model of Hyperammonemia. Frontiers in physiology 2017;8:636. [PubMed: 28912724]

[21]. Azorín I, Miñana M, Felipo V, Grisolía S. A simple animal model of hyperammonemia. Hepatology (Baltimore, Md) 1989;10.

[22]. Formentin C, Zarantonello L, Mangini C, Frigo A, Montagnese S, Merkel C. Clinical, neuropsychological and neurophysiological indices and predictors of hepatic encephalopathy (HE). Liver international : official journal of the International Association for the Study of the Liver 2021;41.

[23]. Montagnese S, Biancardi A, Schiff S, Carraro P, Carlà V, Mannaioni G, et al. Different biochemical correlates for different neuropsychiatric abnormalities in patients with cirrhosis. Hepatology (Baltimore, Md) 2011;53.

[24]. Huizenga J, Gips C, Conn H, Jansen P. Determination of ammonia in ear-lobe capillary blood is an alternative to arterial blood ammonia. Clinica chimica acta; international journal of clinical chemistry 1995;239:65–70. [PubMed: 7586588]

[25]. Granados-Fuentes D, Hermanstyne TO, Carrasquillo Y, Nerbonne JM, Herzog ED. IA Channels Encoded by Kv1.4 and Kv4.2 Regulate Circadian Period of PER2 Expression in the Suprachiasmatic Nucleus. J Biol Rhythms 2015;30:396–407. [PubMed: 26152125]

[26]. Prolo LT JS Herzog ED. Circadian rhythm generation and entrainment in astrocytes. The Journal of neuroscience : the official journal of the Society for Neuroscience 2005;25:404–408. [PubMed: 15647483]

[27]. Abel J, Meeker K, Granados-Fuentes D, St John P, Wang T, Bales B, et al. Functional network inference of the suprachiasmatic nucleus. PNAS 2016;113:4512–4517. [PubMed: 27044085]

[28]. Jones E, Oliphant T, Peterson P. SciPy: Open source scientific tools for Python. 2014.

[29]. Wu G, Anafi R, Hughes M, Kornacker K, Hogenesch J. MetaCycle: an integrated R package to evaluate periodicity in large scale data. Bioinformatics (Oxford, England) 2016;32:3351–3353. [PubMed: 27378304]

[30]. Mönke GS, FA Schmal C; Granada AE. Optimal time frequency analysis for biological data - pyBOAT. bioRxiv 2020.

[31]. Adams KJ, Pratt B, Bose N, Dubois LG, John-Williams LS, Perrott KM, et al. Skyline for Small Molecules: A Unifying Software Package for Quantitative Metabolomics. 2020;19:1447–1458.

[32]. Rose C Effect of ammonia on astrocytic glutamate uptake/release mechanisms - Rose - 2006 - Journal of Neurochemistry - Wiley Online Library. J of Neurochemistry 2006;97 (sel. 1):11–15.

[33]. Ahabrach H, Piedrafita B, Ayad A, El Mlili N, Errami M, Felipo V, et al. Chronic hyperammonemia alters the circadian rhythms of corticosteroid hormone levels and of motor activity in rats. J Neurosci Res 2010;88:1605–1614. [PubMed: 19998493]

[34]. Llansola M, Ahabrach H, Errami M, Cabrera-Pastor A, Addaoudi K, Felipo V. Impaired release of corticosterone from adrenals contributes to impairment of circadian rhythms of activity in hyperammonemic rats. Archives of biochemistry and biophysics 2013;536.

[35]. DeMorrow SC, C Davies N; Jayakumar AR Rose CF. ISHEN guidelines on animal models of hepatic encephalopathy Liver International 2021;41:1474–1478. [PubMed: 33900013]

[36]. Córdoba JD J, Gottstein JB AT. Stenosis of a portacaval anastomosis affects circadian locomotor activity in the rat: a multivariable analysis. American Journal of Phisiology 1997;273:G1218–1225.

[37]. Kim ML EM; Maas MB, Braun RG-C B, Ganger DL DP, Reid KZ PC. Rest-activity rhythm disturbance in liver cirrhosis and association with cognitive impairment. Sleep 2021;44:1–10.

[38]. Montagnese SM B, Mani AS DJ; Morgan MY. Sleep and circadian abnormalities in patients with cirrhosis: features of delayed sleep phase syndrome? Metabolic Brain Disease 2009;24:427–439. [PubMed: 19756996]

[39]. Plotogea OG G, Stan-Ilie MC G; Bacalbasa N; Bungau S, Diaconu C Assessment of Sleep among Patients with Chronic Liver Disease: Association with Quality of Life. Journal of Personalized Medicine 2021;11:1387. [PubMed: 34945859]

[40]. Formentin CG M, Montagnese S Assessment and Management of Sleep Disturbance in Cirrhosis. Current Hepatology Reports 2018;17:52–69. [PubMed: 29876197]

[41]. Markham C, Williams C, Miller C, Grange D, Davis T, Remy K. Continuous Renal Replacement Therapy for Two Neonates With Hyperammonemia. Frontiers in pediatrics 2021;9:1–7.

[42]. Bergonzi PB A; Mazza S; Mennuni G; Zolo P Organization of nocturnal sleep in patients with liver cirrhosis: changes before and after treatment with levodopa and lactulose. Rivista di neurologia 1975;45:118–123. [PubMed: 167416]

[43]. Cordoba J, Steindl P, Blei A. Melatonin arrhythmia is corrected after liver transplantation. The American journal of gastroenterology 2009;104:1862–1863.

[44]. Giva S, Finnegan J, Ihidero P, Maguire G, Power B, Knerr I, et al. Hyperammonaemia in Neonates and Young Children: Potential Metabolic Causes, Diagnostic Approaches and Clinical Consequences. Irish medical journal 2019;112:858. [PubMed: 30719899]

[45]. Abbott SM, Reid KJ, Zee PC. Circadian Rhythm Sleep-Wake Disorders. Psychiatric Clinics of North America 2015;38:805-+. [PubMed: 26600110]

[46]. De Rui M, Middleton B, Sticca A, Gatta A, Amodio P, Skene D, et al. Sleep and circadian rhythms in hospitalized patients with decompensated cirrhosis: effect of light therapy. Neurochemical research 2015;40:284–292. [PubMed: 25135598]

[47]. Turco M, Cazzagon N, Franceschet I, Formentin C, Frighetto G, Giordani F, et al. Morning Bright Light Treatment for Sleep-Wake Disturbances in Primary Biliary Cholangitis: A Pilot Study. Frontiers in physiology 2018;9:1530. [PubMed: 30455647]

[48]. Shinohara K, Honma S, Katsuno Y, Honma K. Circadian release of excitatory amino acids in the suprachiasmatic nucleus culture is Ca(2+)-independent. Neuroscience research 2000;36.

[49]. Shinohara K, Honma S, Katsuno Y, Abe H, Honma K. Circadian release of amino acids in the suprachiasmatic nucleus in vitro. Neuroreport 1998;9.

[50]. Cabrera-Pastor AB T, Hernández-Rabaza VM M; Llansola M; Felipo V;. Increasing extracellular cGMP in cerebellum in vivo reduces neuroinflammation, GABAergic tone and motor in-coordination in hyperammonemic rats. Brain, behavior, and immunity 2018;69:386–398. [PubMed: 29288802]

[51]. Monfort P, Muñoz M, ElAyadi A, Kosenko E, Felipo V. Effects of hyperammonemia and liver failure on glutamatergic neurotransmission. Metabolic brain disease 2002;17:237–250. [PubMed: 12602501]

[52]. Schroeter A, Wen S, Mölders A, Erlenhardt N, Stein V, Klöcker N. Depletion of the AMPAR reserve pool impairs synaptic plasticity in a model of hepatic encephalopathy. Molecular and cellular neurosciences 2015;68:331–339. [PubMed: 26363416]

[53]. Taoro-Gonzalez L, Arenas Y, Cabrera-Pastor A, Felipo V. Extracellular cGMP Reverses Altered Membrane Expression of AMPA Receptors in Hippocampus of Hyperammonemic Rats: Underlying Mechanisms. Molecular neurobiology 2019;56. [PubMed: 29675577]

[54]. Sancho-Alonso M, Taoro-Gonzalez L, Cabrera-Pastor A, Felipo V, Teruel-Martí V. Hyperammonemia Alters the Function of AMPA and NMDA Receptors in Hippocampus: Extracellular cGMP Reverses Some of These Alterations. Neurochemical research 2022;47.

[55]. Kumamoto A, Chiba Y, Suda A, Hishimoto A, Kase A. A Severe Dementia Case in End of Life Care with Psychiatric Symptoms Treated by Perampanel. Journal of epilepsy research 2021;11.

[56]. Llansola M, Rodrigo R, Monfort P, Montoliu C, Kosenko E, Cauli O, et al. NMDA receptors in hyperammonemia and hepatic encephalopathy. Metabolic brain disease 2007;22:321–335. [PubMed: 17701332]

[57]. Arenas Y, Martínez-García M, Llansola M, Felipo V. Enhanced BDNF and TrkB Activation Enhance GABA Neurotransmission in Cerebellum in Hyperammonemia. International journal of molecular sciences 2022;23. [PubMed: 36613467]

[58]. Aldridge D, Tranah E, Shawcross D. Pathogenesis of hepatic encephalopathy: role of ammonia and systemic inflammation. Journal of clinical and experimental hepatology 2015;5.

[59]. Rodrigo R, Cauli O, Gomez-Pinedo U, Agusti A, Hernandez-Rabaza V, Garcia-Verdugo J, et al. Hyperammonemia induces neuroinflammation that contributes to cognitive impairment in rats with hepatic encephalopathy. Gastroenterology 2010;139. [PubMed: 21108823]

[60]. Montagnese S, Lauridsen M, Vilstrup H, Zarantonello L, Lakner G, Fitilev S, et al. A pilot study of golexanolone, a new GABA-A receptor-modulating steroid antagonist, in patients with covert hepatic encephalopathy. Journal of hepatology 2021;75. [PubMed: 34487750]

[61]. Butterworth R Hepatic Encephalopathy in Cirrhosis: Pathology and Pathophysiology. Drugs 2019;79.

[62]. Cabrera-Pastor A, Arenas Y, Taoro-Gonzalez L, Montoliu C, Felipo V. Chronic hyperammonemia alters extracellular glutamate, glutamine and GABA and membrane expression of their transporters in rat cerebellum. Modulation by extracellular cGMP. Neuropharmacology 2019;161. [PubMed: 30797029]

Key Points

- Mice fed a hyperammonaemic diet advanced their daily activity onset time by ~1 hour and decreased their total activity, concentrating it during the first half of the night.

- Ammonia significantly increased extracellular glutamate and reduced the circadian amplitude and synchrony of circadian cells, in suprachiasmatic nuclei (SCN) explants.

- The ammonia-induced decrease in amplitude of the SCN was reversed by ammonia removal or by AMPA glutamate receptor antagonists.
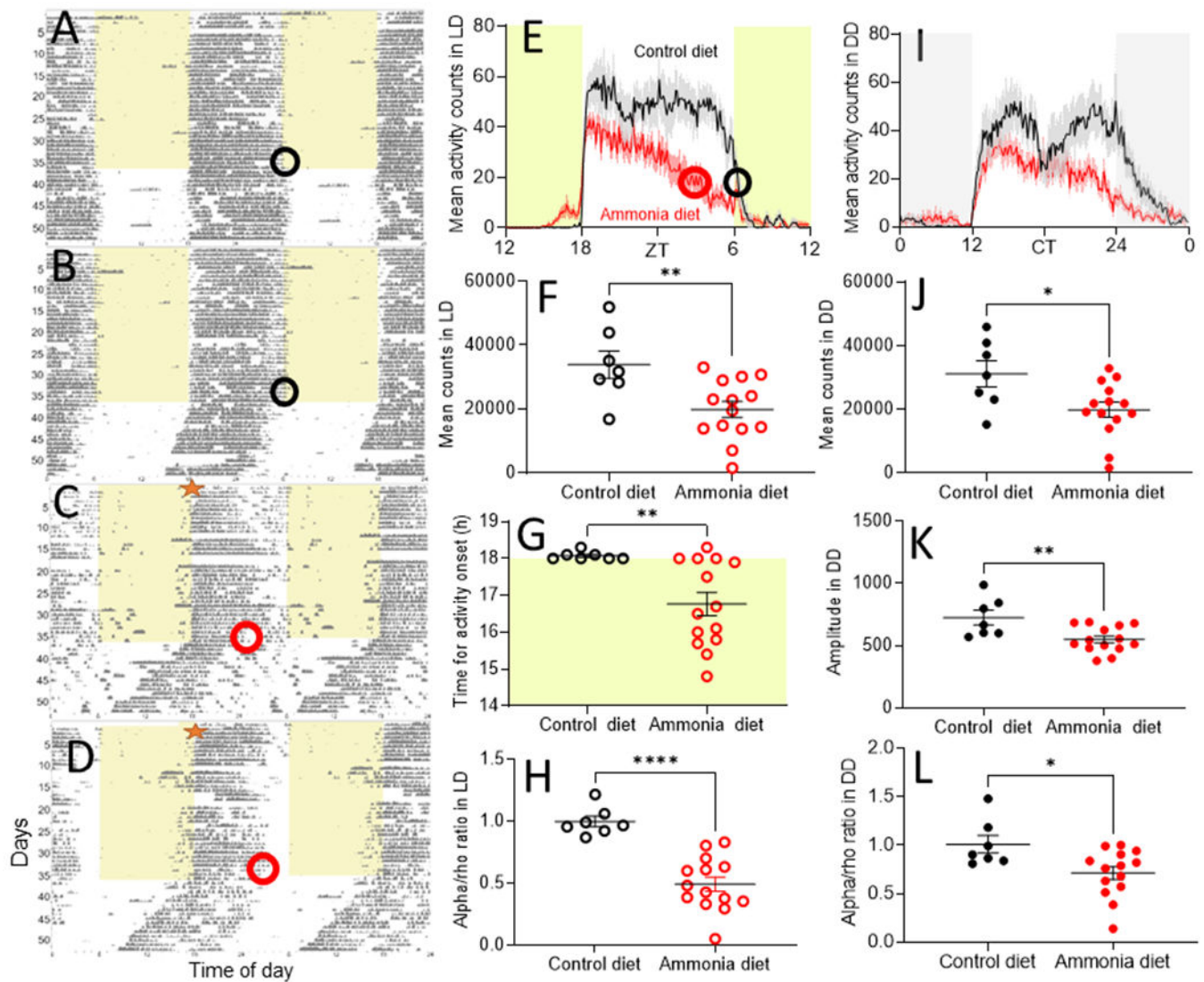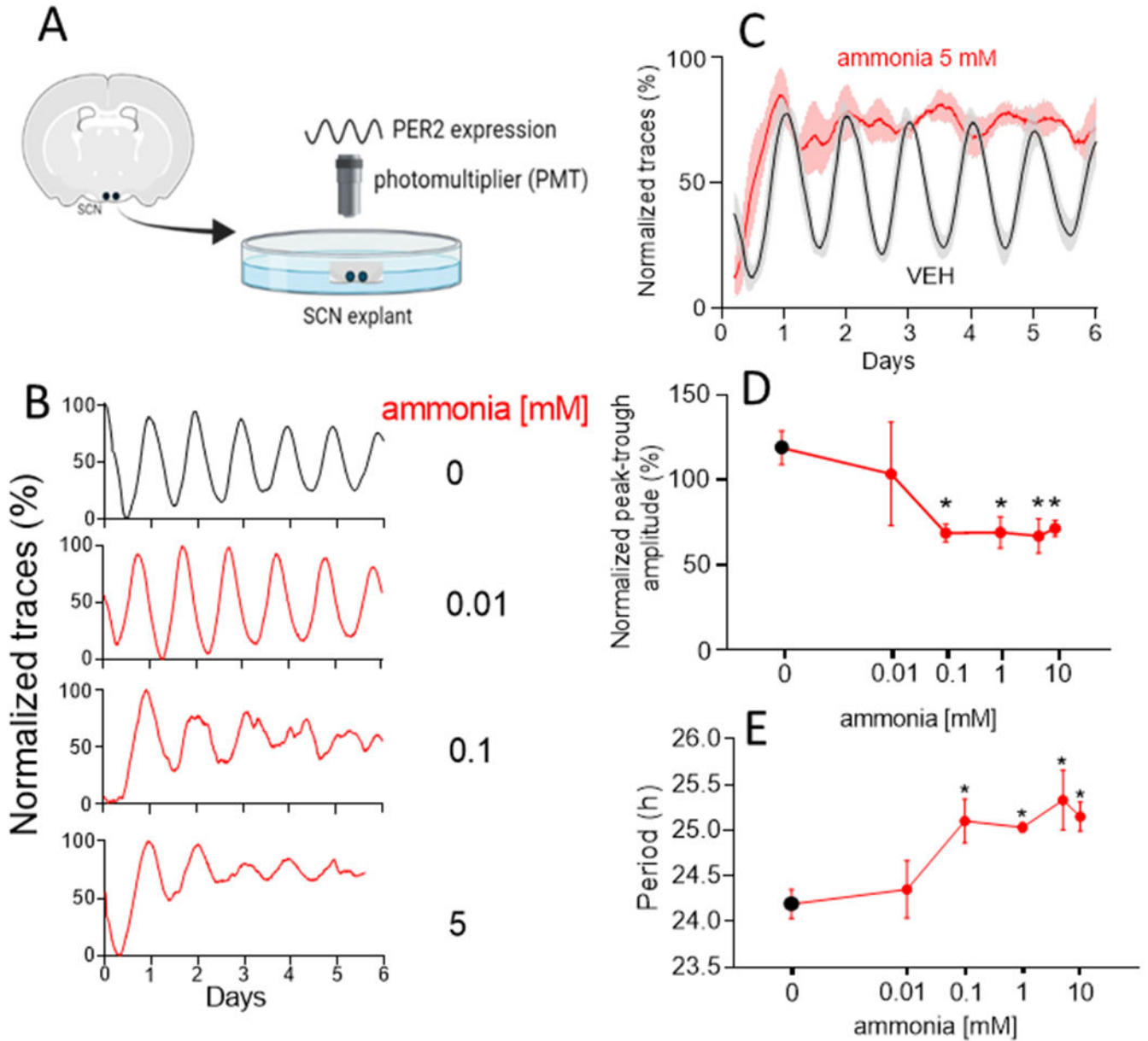
Figure 1. Hyperammonaemic diet affected running-wheel activity.
Representative running-wheel actograms of mice receiving control (A, B, n = 7) or hyperammonaemic diet (C, D, n = 13). Empty black or red circles on the actograms (A-D) show the days analysed or the end of the mean activity (E). Hyperammonaemic diet was available ad-lib from the beginning of the recording (red star on C and D). Under dim LD conditions, mice receiving the hyperammonaemic diet were active mostly during the first half (from ~Zeitgeber Time 18-24) of the activity phase (E and G, ****p<0.001) with an advanced onset of activity (E and H, **p=0.009) and lower total activity (F, **p=0.007). Under DD conditions (I), hyperammonaemic mice also showed decreased activity counts (J, *p=0.02), decreased in amplitude (K, **p=0.007) and decreased alpha/rho ratio (L, *p=0.02).
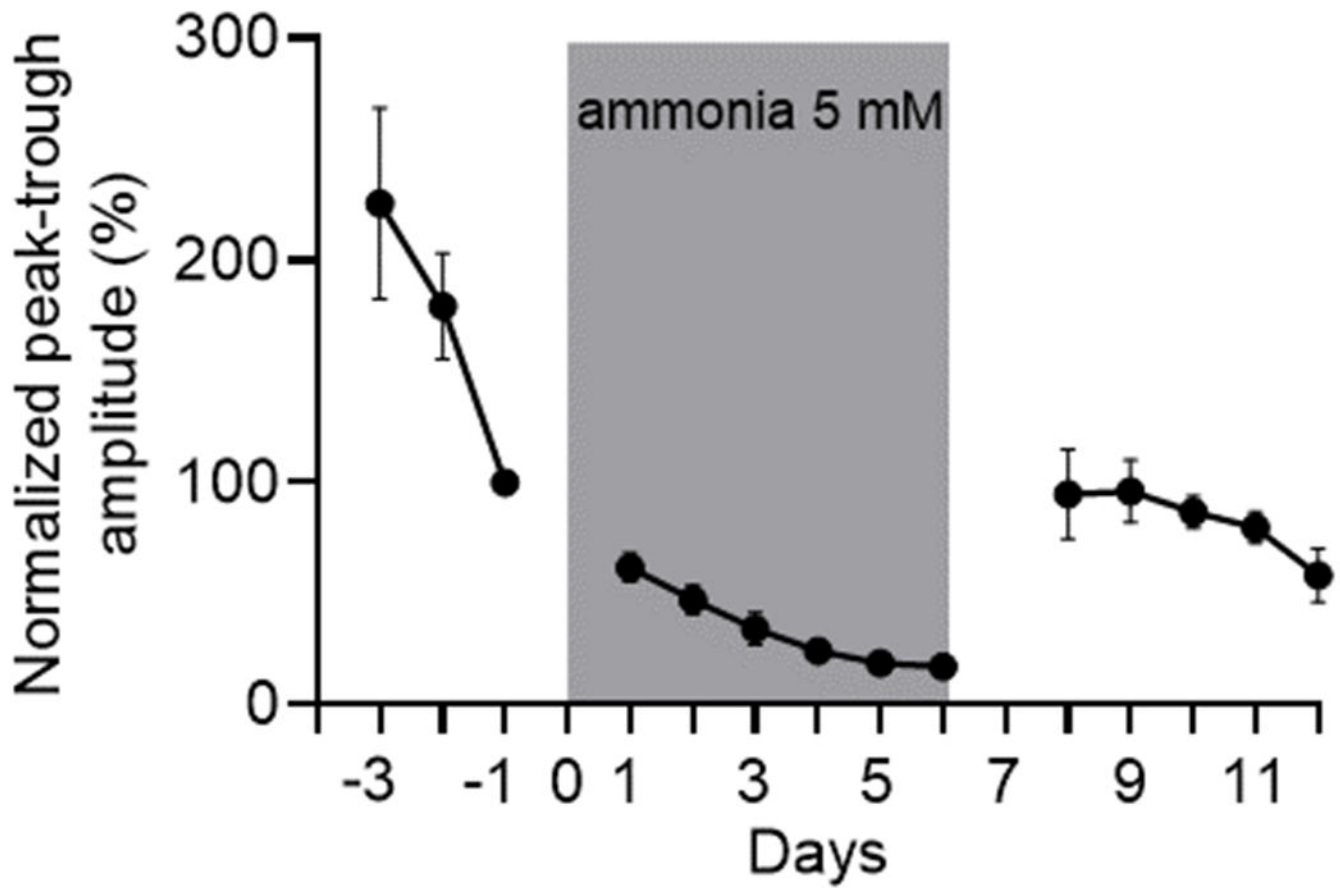
Figure 2. Ammonia decreased amplitude and increased period of PER2 expression in adult SCN.
(A) Schematic methodology: SCN explants from a Per2[Luc] mouse producing the
PERIOD2::LUCIFERASE fusion protein as a reporter of PER2 expression were cultured on
organotypic membranes inside Petri dishes from which bioluminescence was recorded using
photomultiplier tubes (PMT). (B) PER2 expression single traces from adult SCN explants
in vehicle (VEH; n=11) and three representative ammonia concentrations (n=6-10) along six
days of recording. (C) Mean±SEM group trace comparisons for VEH (continuous line) and
ammonia 5 mM (dashed line). (D) Ammonia induced a reduction in amplitude measured
at the second day of recording of ~80% at and above ammonia 0.1 mM (*p=0.002) while
period (E) was increased also at and above ammonia 0.1 mM (*p=0.003).

Figure 3. Ammonia effect on PER2 amplitude in adult SCN was reversible.
Peak-trough PER2^{LUC} expression amplitude returned to baseline levels after ammonia 5 mM (n=5) was washed. Ammonia remained in the culture media from day 0 to day 6 (grey rectangle) and then washed out on day 7. Amplitude was normalized to day -1.
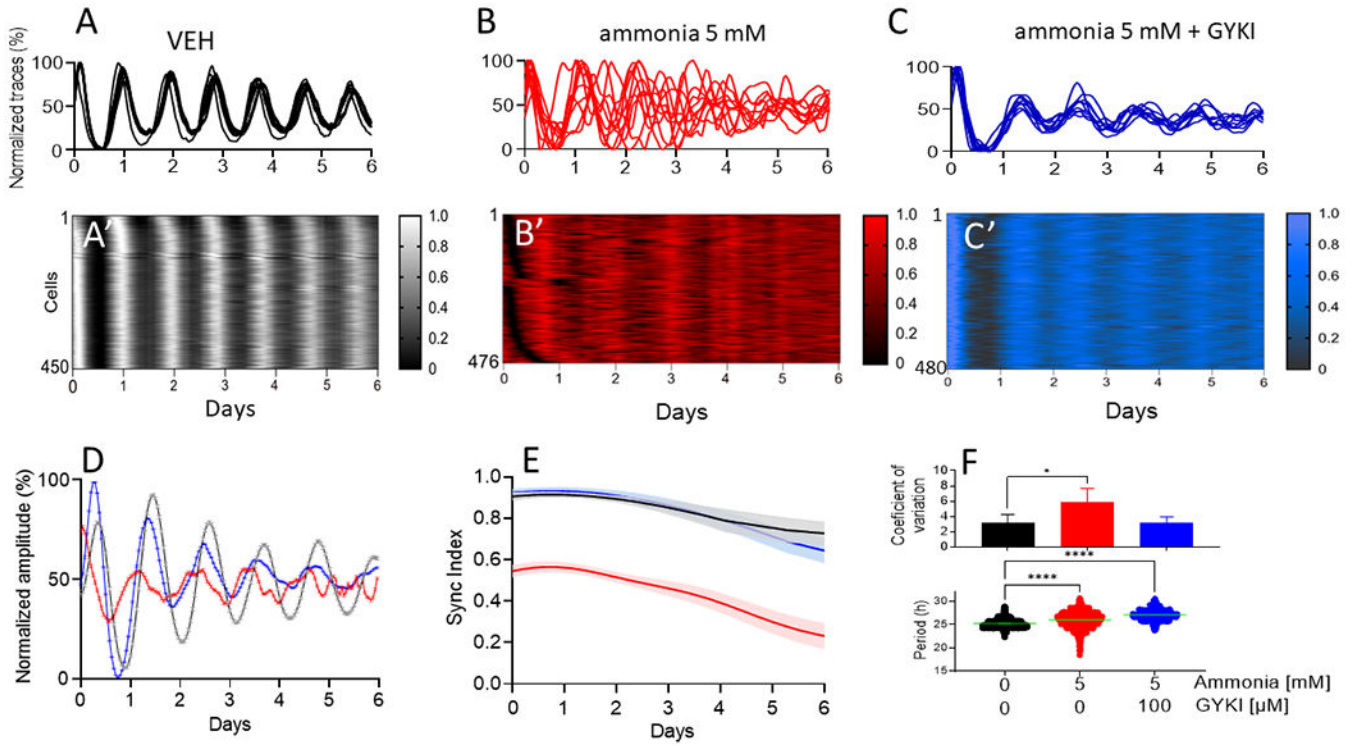
Figure 4. Ammonia induced desynchrony among single cells in adult SCN which was prevented by AMPA receptors blocking.

Representative single cell traces of PER2^{LUC} expression in VEH (A, n=6), ammonia 5 mM (B, n=6) and ammonia 5mM + GYKI 100 μM (C, n=4) with their respective raster plots (A', B' and C') depicting all cells from a representative single SCN explant showing desynchrony induced by ammonia that was prevented by GIKI application. (D) Ensemble mean±SEM PER2^{LUC} expression traces from the same single SCN explants. (E) Group mean±SEM sync indices showing that high synchrony among SCN cells was re-stablished when AMPA receptors were blocked with GYKI. (F) Ammonia increased period (lower panel, *p>0.001) of single SCN cells which was correlated with an increase in the coefficient of variation (top panel, *p=0.03).
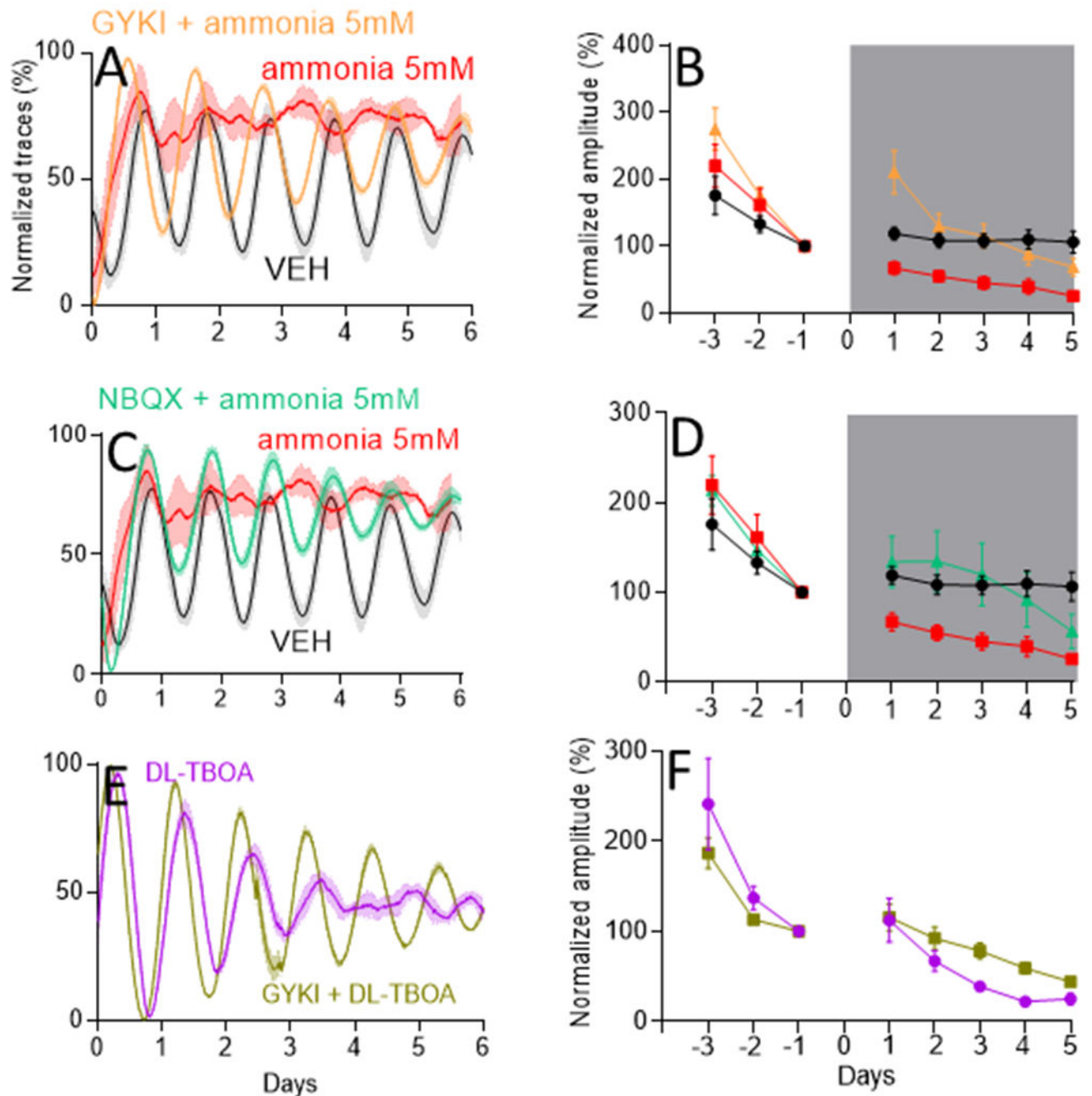
Figure 5. Ammonia induced decrease in PER2 amplitude in the SCN was prevented by AMPA receptors blocking.
(A) mean±SEM PER2^{LUC} expression traces of VEH (n=12), ammonia 5 mM (n=11) and ammonia 5 mM + GYKI 100 μM (n=13) groups with their respective PER2^{LUC} amplitudes (B). (C) same as (A) but with ammonia 5 mM and NBQX 100 μM (n=5) with their respective amplitudes in (D). Both AMPA blockers prevented decrease in PER2^{LUC} amplitude induced by ammonia (p=0.5 for both). For B and D amplitude was normalized to day −1.